Enhanced amino acid utilization sustains growth of cells lacking Snf1/AMPK

Biochimica et Biophysica Acta 1853 (2015) 1615–1625

Contents lists available at ScienceDirect

Biochimica et Biophysica Acta

journal homepage: www.elsevier.com/locate/bbamcr

Enhanced amino acid utilization sustains growth of cells lacking Snf1/AMPK

Raffaele Nicastro [a,b], Farida Tripodi [a,b], Cinzia Guzzi [a,b], Veronica Reghellin [a,b], Sakda Khoomrung [c], Claudia Capusoni [e], Concetta Compagno [e], Cristina Airoldi [a,b], Jens Nielsen [c,d], Lilia Alberghina [a,b], Paola Coccetti [a,b,*]

[a] SYSBIO, Centre of Systems Biology, Milan, Italy
[b] Department of Biotechnology and Biosciences, University of Milano-Bicocca, Milan, Italy
[c] Department of Chemical and Biological Engineering, Chalmers University of Technology, Gothenburg, Sweden
[d] Novo Nordisk Foundation Center for Biosustainability, Technical University of Denmark, Hørsholm, Denmark
[e] Department of Food, Environmental and Nutritional Sciences, University of Milan, Milan, Italy

ARTICLE INFO

Article history:
Received 3 January 2015
Received in revised form 16 March 2015
Accepted 25 March 2015
Available online 2 April 2015

Keywords:
Saccharomyces cerevisiae
Glucose
Budding yeast
Metabolism
Respiration
Gene chip

ABSTRACT

The metabolism of proliferating cells shows common features even in evolutionary distant organisms such as mammals and yeasts, for example the requirement for anabolic processes under tight control of signaling pathways. Analysis of the rewiring of metabolism, which occurs following the dysregulation of signaling pathways, provides new knowledge about the mechanisms underlying cell proliferation.
The key energy regulator in yeast Snf1 and its mammalian ortholog AMPK have earlier been shown to have similar functions at glucose limited conditions and here we show that they also have analogies when grown with glucose excess. We show that loss of Snf1 in cells growing in 2% glucose induces an extensive transcriptional reprogramming, enhances glycolytic activity, fatty acid accumulation and reliance on amino acid utilization for growth. Strikingly, we demonstrate that Snf1/AMPK-deficient cells remodel their metabolism fueling mitochondria and show glucose and amino acids addiction, a typical hallmark of cancer cells.

1. Introduction

All proliferating cells need to match growth and cell cycle progression with nutrient availability to maintain cell size homeostasis [1,2]. Since duplication requires the doubling of all cellular macromolecules, including proteins, nucleic acids and lipids, the major issue for dividing cells is the increase in biomass and thus the coordinated performance of anabolic processes [3].

One of the major challenges to better understand the metabolism of proliferating cells is its integration with signal transduction pathways. One of such pathways is centered on the AMP-activated protein kinase (AMPK), an evolutionary conserved regulator of cellular energy homeostasis in eukaryotes [4]. AMPK is activated by an increase in AMP levels, which signals a decrease in energy production, and executes an energy-saving program by inhibiting protein, carbohydrate and lipid synthesis, resulting in cell growth and proliferation being switched off [4].

Protein kinase Snf1, the homolog of AMPK in *Saccharomyces cerevisiae*, shares evolutionary conserved features with its counterparts in other eukaryotes, such as the heterotrimeric structure of the holoenzyme and the deep involvement in energy preservation [5]. Snf1 is responsible for direct phosphorylation of metabolic enzymes, for example it phosphorylates and inactivates the glycerol-3-phosphate dehydrogenase isoform Gpd2 [6] and the acetyl-CoA carboxylase Acc1 [7], in both cases to preserve the central carbon metabolism from wasteful processes when nutrients are scarce.

Snf1 catalytic activity is of primary importance in yeast for the growth in the presence of low glucose and the utilization of alternative carbon sources, mainly because it mediates the de-repression of a large regulon of genes normally inhibited by the transcriptional repressor Mig1 when nutrients are in excess [8]. Therefore, in the past the kinase has been mostly studied at nutrient limited condition [9–12].

Recently we identified a role for Snf1 in cells grown in 2% glucose, condition that supports maximal growth rate, showing its involvement in the regulation of the G_1/S transition of the cell cycle [13,14]. It is therefore evident that Snf1 plays a role even when cells are not under stress conditions, like nutrient limitation, but also when cells grow in a favorable environment for proliferation.

Here we dissect how the metabolic profile of yeast cells is affected by loss of Snf1 both in 2% and 5% glucose, showing several features of the metabolic rewiring occurring because of the impairment of a signaling

* Corresponding author at: Department of Biotechnology and Biosciences, University of Milano-Bicocca, Milan, Italy. Tel.: +39 0264483521.
E-mail address: paola.coccetti@unimib.it (P. Coccetti).

http://dx.doi.org/10.1016/j.bbamcr.2015.03.014
0167-4889/

pathway controlling single metabolic steps. Moreover, we present evidences that indicate that the maximal growth rate in 2% glucose is obtained by *snf1*Δ cells enhancing the utilization of amino acids supplemented in the medium, which is no longer mandatory in 5% glucose.

Our study supports the usefulness of yeast as model organism for the study of the metabolism of proliferating eukaryotic cells and in particular for those with alterations in the AMPK signaling pathway.

2. Materials and methods

2.1. Yeast strains and growth conditions

S. cerevisiae strains used in this study are isogenic to BY4741 and are reported in Table 1. Synthetic medium contained 2% glucose or 5% glucose, 6.7 g/L of Yeast Nitrogen Base (Difco), 50 mg/L of required nutrients, at standard pH (5.5). In these conditions cells exhibit exponential growth between OD_{600nm} = 0.1 ($2*10^6$ cells/mL) and OD_{600nm} = 1.5 ($3*10^7$ cells/mL). Cell density of liquid cultures grown at 30 °C was determined with a Coulter counter on mildly sonicated and diluted samples or spectrophotometrically at 600 nm. All analyses were performed at cell densities between OD_{600nm} = 0.1 ($2*10^6$ cells/ml) and OD_{600nm} = 0.7 ($1.3*10^7$ cells/ml). Antimycin A (Sigma) was added at a final concentration of 1 μg/ml (from a 2 mg/ml stock in 100% ethanol); as a control, a culture grown in the presence of the same concentration of ethanol was used. For experiments with the Snf1(I132G)^{as} strain, 25 μM 2NM-PP1 (from a 25 mM stock in 100% DMSO) was added to inhibit the activity of Snf1 [10]; as a control, a culture grown in the presence of the same concentration of solvent (0.1% DMSO) was used. Synthesis of compound 2NM-PP1 was carried out as previously described [14].

2.2. Gene Chip® analysis

Total RNA concentration and purity of yeast samples was assessed by spectrophotometer (Nanodrop) evaluating $260_{nm}/280_{nm}$ and $260_{nm}/230_{nm}$ ratios. Total RNA integrity was assessed by Agilent Bioanalyzer. An aliquot (300 ng) of RNA was used for the preparation of targets for Affymetrix® Yeast Genome 2.0 arrays, according to the Ambion MessageAmp III RNA amplification kit manual. Affymetrix® Yeast Genome 2.0 arrays (which contain 10928 genes) were purchased from Affymetrix (Affymetrix, USA). The staining, washing and scanning of the arrays were conducted using the Fluidics 450 station, Command Console Software and GeneChip® Scanner 3000 7G, generating.CEL files for each array (Affymetrix, USA). The images were scanned by Affymetrix GeneChip Command Console (AGCC) and analyzed with the Affymetrix GeneChip Expression Console. The quality control of the scanned data was first estimated by confirming the order of the signal intensities of the Poly-A and Hybridization controls using Expression Console Software (Affymetrix, USA). Raw expression values were imported as Affymetrix.CEL files into Partek Genomics Suite 6.6 (Partek Inc., St. Louis, MO, USA), were analyzed and normalized, including the Preprocessing, Differentially Expressed Genes (DEGs) Finding and Clustering modules. The.CEL files were uploaded and normalized in PM (perfect match)-only conditions as a PM intensity adjustment. A Robust Multichip Analysis (RMA) quantification method [15] was used as a probe set summarization algorithm for log transformation with base 2 (log2) and the Quantile normalization method was chosen to evaluate the preliminary data quality in the Preprocessing module, which functions as a data quality control through the Affymetrix Expression Console Software. The mean signal intensities of all genes were obtained using a group of arrays for each condition. After normalization, the differentially expressed genes (DEGs) satisfying the conditions of the Fold Change settings (FC = ± 1.5) from all of the genes probed in the array were selected in the DEGs Finding module. Hierarchical cluster analysis was also performed to see how data aggregated and to generate heat maps. The obtained data were stored in the ArrayExpress database, accession number E-MTAB-3190.

Table 1
Yeast strains used in this work.

Strain	Genotype	Origin
BY wt	*MATa his3Δ1 leu2Δ0 met15Δ0 ura3Δ0*	Open Biosystems
snf1Δ	*MATa his3Δ1 leu2Δ0 met15Δ0 ura3Δ0 snf1::HPH*	This study
Snf1^{as}	*MATa his3Δ1 leu2Δ0 met15Δ0 ura3Δ0 snf1::HPH [pRS316-SNF1-I132G-3HA (URA3)]*	[14]

All strains are isogenic to BY4741.

2.3. RNA purification and qReal-time PCR

Total RNA was isolated using a phenol-chloroform protocol, essentially as previously described [13]. Reverse transcription of 0.5 μg of total RNA was carried out with iScript cDNA Synthesis Kit (BIO-RAD). Quantitative Real-time PCR for gene expression was performed using SsoFast EvaGreen Supermix (BIO-RAD), oligos available upon request. Obtained data were normalized to both *ACT1* and *CDC34* reference genes and organized with CFX manager software (Bio-Rad), which provided statistical analysis. Data are presented as the mean value ± standard deviation from at least three independent experiments performed in technical duplicates.

2.4. Metabolites extraction and analysis

Metabolic profiling by ^{1}H-NMR of intracellular and extracellular metabolites was performed as previously described [16]. Fatty acids were extracted and analyzed by GC-MS as in [17]. Analysis of intracellular organic acids was carried out as in (Khoomrung et al., in preparation). Briefly, organic acids were extracted from 3–10 mg of dried biomass with a 50:50 mixture of aqueous methanol (50% MeOH, 50% H_2O) and chloroform. After vortexing at 2000 r.p.m. for 45 min at −20 °C and centrifugation, the aqueous phase was recovered and evaporated. The metabolites were resuspended in 400 μl acetonitrile and 100 μl tert-butyldimethylsilane (TBDMS, Sigma-Aldrich) and derivatization was carried out for 2 hours at 80 °C. GC-MS analysis was performed with a Focus GC ISQ single quadrupole GC-MS (Thermo Fisher scientific, USA). Quantification of each compound was performed using calibration curves prepared with specific standards. Extracellular levels of glucose, ethanol, acetate and amino acids were evaluated by ^{1}H-NMR on growth media as reported [16].

2.5. ATP and NAD^+/NADH assays

ATP was measured using the CellTiter-Glo® Luminescent Assay (Promega) following the manufacturer's instructions, using 100 μl of a OD_{600nm} = 0.3 culture. NAD^+ and NADH were measured using the EnzyChrom™ NAD/NADH Assay Kit (Medibena), following the manufacturer's instructions.

2.6. Enzymatic assays

For enzymatic assays, cells at OD_{600nm} = 0.3 were rapidly collected by filtration and frozen at −80 °C. Total protein extracts were obtained disrupting the cells with glass beads in the buffer appropriate for each assay, protein concentrations were determined using the Bio-Rad protein assay (Bio-Rad) and enzymatic assays were performed on equal amount of protein extracts. Hexokinase activity was assayed essentially as previously described [18]. Enolase and isocitrate dehydrogenase activities were assayed essentially as described [18]. Malate dehydrogenase was assayed essentially as previously described [18]. Glyceraldehyde-3-phosphate dehydrogenase activity assay was

performed essentially as described [19]. Glucose-6-phosphate dehydrogenase activity was measured essentially as in [20]. Isocitrate lyase activity was assayed as in [21]. Glutamate synthase (GOGAT) activity was assayed as in [22]. Glutamic dehydrogenase activity was assayed essentially as in [23].

2.7. Oxygen consumption measurement

Oxygen consumption rates were measured according to [24] with few modifications. Briefly, cells were inoculated in 2% or 5% glucose containing medium and when they reached the exponential growth phase ($OD_{600nm} = 0.5$), the respiratory rate was measured at room temperature in growth media using a calibrated Clark-type electrode (Mettler Toledo). The respiratory rate qO2 was expressed as $mmol_{oxygen} min^{-1} g^{-1}_{dry\ weight}$.

2.8. Statistical analyses

Experiments were carried out at least in biological triplicate. Results are expressed as mean ± SD and compared using the two-sided Student's (t-test). * $p < 0.05$, ** $p < 0.005$ and *** $p < 0.0005$.

3. Results

3.1. Deletion of SNF1 causes a large transcriptional reprogramming in cells growing in 2% glucose

Protein kinase Snf1 is known for its role in response to stress conditions and nutrient limitations [5]. We recently highlighted its requirement also for growth and cell cycle progression at standard glucose growth condition (2% glucose), requirement that disappeared with a larger (5%) glucose supply [13,14]. To characterize the poor growth phenotype of *snf1Δ* cells in a 2% glucose synthetic medium, we performed transcriptome analysis (Affymetrix) of wild type and *snf1Δ* cells growing in this condition, as well as in 5% glucose.

snf1Δ cells growing in 2% glucose showed extensive transcriptional reprogramming as compared to the wild type, involving about 1000 genes, with a slight predominance of up-regulated transcripts (Fig. S1A). Increasing the glucose concentration to 5% greatly reduced the number of differentially expressed genes to roughly 300 (Fig. 1A). Strikingly, the DEGs (differential expressed genes) in 5% glucose resulted mostly in a subset of the DEGs in 2% glucose (Fig. 1A) and highly correlated with these, but with reduced fold changes (Fig. 1B). This finding indicates that the loss of the slow-growth phenotype of *snf1Δ* cells with higher glucose availability correlates with the reversion of the differential gene expression.

Gene Ontology enrichment analysis of the up-regulated transcripts in *snf1Δ* cells growing in 2% glucose showed de-repression of genes involved mainly in transmembrane transport and in a large number of metabolic processes (Figs. S1B and S1C). In particular, more than 100 up-regulated genes encoded for transmembrane transporters of amino acids and other metabolites, mostly targets of the Gcn4 transcription factor (Fig. S1B). Interestingly, the inhibition of Snf1 catalytic activity has been shown to cause the de-repression of Gcn4-regulated genes through the regulation of translation of the transcription factor in cells growing in low glucose [10]. Our data indicate that this phenomenon could be extended also to glucose-repressed cells, further supporting the emerging role of Snf1 also in non-limiting nutrient conditions. The major part of the remaining up-regulated genes was involved in several metabolic processes such as redox metabolism, iron homeostasis and amino acids biosynthesis (Fig. S1C). Further analysis of the subset of up-regulated genes in *snf1Δ* cells growing in 2% glucose for enrichment in KEGG pathways remarkably identified metabolic processes not previously linked to Snf1, overall glycolysis/gluconeogenesis and associated sugar metabolisms, as well as known Snf1-controlled pathways such as fatty acid metabolism (Fig. 1C). Gene Ontology enrichment of down-regulated genes revealed that the presence of Snf1 is required for the expression of genes important for mitochondrial functionality and cell cycle progression (Fig. S1D). In particular, several genes coding for structural proteins of both the small and large subunits of the mitochondrial ribosomes were down-regulated in *snf1Δ* cells grown in 2% glucose, as well as cell cycle-related genes, mainly involved in microtubule assembly and mitosis (Fig. S1D).

Notably, genes involved in phosphate metabolism present an interesting response in expression between 2% and 5% glucose in *snf1Δ* cells. Genes coding for high affinity phosphate transporters (*PHO84* and *PHO89*), the membrane glycoprotein *PHO11* and the transcription factor *SPL2* were inhibited by the deletion of *SNF1* in 2% glucose, while the *PHO87* gene coding for the low affinity transporter was up-regulated in the same condition (Fig. S1B). The same genes switched behavior in 5% glucose, possibly indicating that the restored growth due to the higher glucose availability was sensed as not matched by sufficient phosphate uptake.

Taken together, these data provide a wide picture of the transcriptional re-arrangement occurring in cells lacking Snf1 in a condition in which the activity of the kinase is not essential for the de-repression of genes subject to catabolite repression but guarantees a proper growth, as well as in the presence of a larger glucose supply (5% glucose) in which the presence of Snf1 becomes dispensable.

3.2. Deletion of SNF1 or inhibition of Snf1 catalytic activity causes the up-regulation of several glycolytic genes

Snf1 is known to regulate the transcription of several metabolic genes, enhancing the expression of enzymes involved in the utilization of low glucose levels or of alternative carbon sources [5]. Here we show that Snf1 also functions as a regulator of glycolytic genes as there is de-repression of several of these genes in *snf1Δ* cells growing in 2% glucose (Fig. 1D). To validate this finding we performed real-time PCR analyses of glycolytic genes mRNAs, confirming the up-regulation of *TDH1* and *ENO1*, while *HXK1* was downregulated (Fig. 1E). In the previous section, we highlighted that the loss of the growth defect of *snf1Δ* cells in 5% glucose was accompanied by a consistent normalization of the transcriptional phenotype (Fig. S1A). This phenomenon was confirmed also for glycolytic genes, since all of them showed nearly wild type expression levels in 5% glucose (Fig. 1E).

To demonstrate that the de-repression of glycolytic genes was specifically due to the lack of Snf1 catalytic activity, we used a strain carrying an analog sensitive isoform of Snf1 (Snf1-I132G), which activity can be inhibited by the ATP analog 2NM-PP1 [10,14] and checked the mRNA levels of representative genes following addition of 2NM-PP1 (Fig. 1F). Higher levels of *TDH1* and *ENO1* mRNAs were detectable already after 1 hour following treatment with the inhibitor, with an even higher expression after 2 hours (Fig. 1F).

Altogether, these data demonstrate that Snf1 catalytic activity is required for the transcriptional repression of glycolytic genes and, more intriguingly, that this response is performed in a glucose-dependent fashion.

3.3. Lack of Snf1 causes enhanced secretion of fermentation products

Transcription of glycolytic genes has been reported to influence the enzymatic activity of the corresponding gene products, as shown using strains lacking the transcription factor Gcr1 or the co-activator Gcr2 [25]. We therefore wondered whether the observed transcriptional up-regulation resulted in higher activity of glycolytic enzymes. Surprisingly, we were unable to detect significant variations of the activity of hexokinase (HXK), glycerahldehyde-3-phosphate dehydrogenase (GPDH) and pyruvate kinase (Pyr Kinase) (Fig. 2A).

To determine whether glycolysis was altered in *snf1Δ* cells, we measured the glucose consumption in log phase cultures by NMR spectroscopy. Interestingly, glucose uptake of the mutant strain was at

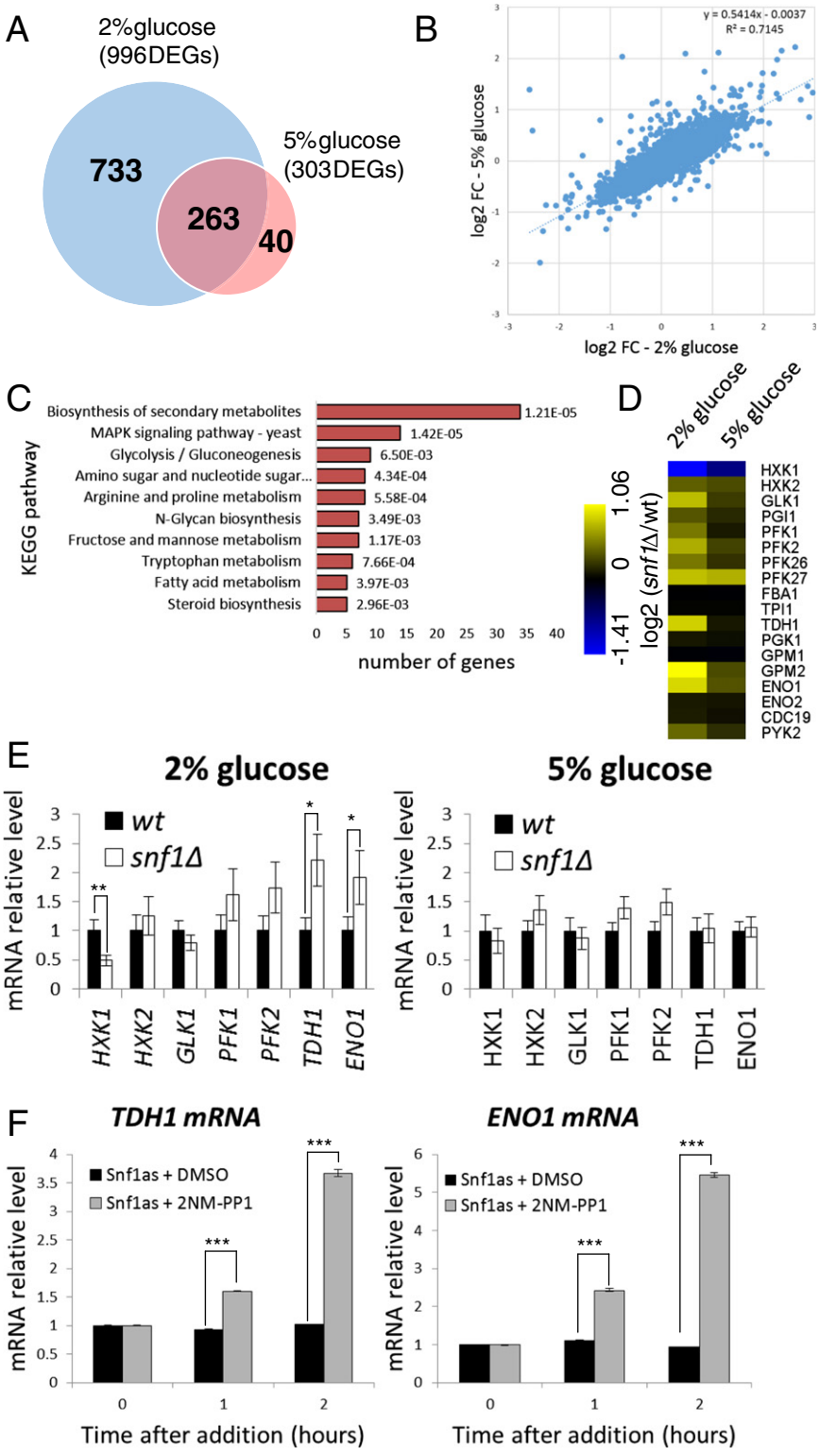

Fig. 1. Transcriptional reprogramming of *snf1Δ* yeast cells growing in 2% glucose. (A) Euler diagram showing the overlap between the differential expressed genes (DEGs) in *snf1Δ* batch cultures (culture density $OD_{600nm} = 0.3$) supplemented either with 2% or 5% glucose, compared to the wt. (B) Dot-plot of the correlation of the fold change of DEGs in the *snf1Δ*/wt 2% glucose and *snf1Δ*/wt 5% glucose comparisons. (C) KEGG Pathways enrichment of the up-regulated genes in *snf1Δ* cells growing in 2% glucose compared to the wt. Enrichment p-value is shown beside each bar. (D) Heat map showing the log2 fold change of expression of glycolytic genes in *snf1Δ* cells growing in 2% and 5% glucose, compared to the wt. (E) Real-time PCR quantification of mRNAs of the indicated genes in wt and *snf1Δ* cells growing respectively in 2% glucose and 5% glucose (culture density $OD_{600nm} = 0.3$). *p-value < 0.05; **p-value < 0.005. (F) Real-time PCR quantification of *TDH1* and *ENO1* mRNAs in the $Snf1^{as}$ strain following treatment with 2NM-PP1, DMSO was used as control. ***p-value < 0.0005.

wt levels in 2% glucose (consumption shown as a function of culture density), but was appreciably higher, as compared to the wt, in 5% glucose (Fig. 2B). The unaltered glucose uptake in 2% glucose was surprising, given the up-regulation of the gene coding for the high capacity glucose transporter Hxt1 which depends on the impairment of a known transcriptional regulation exerted by Snf1 [26]. Nevertheless,

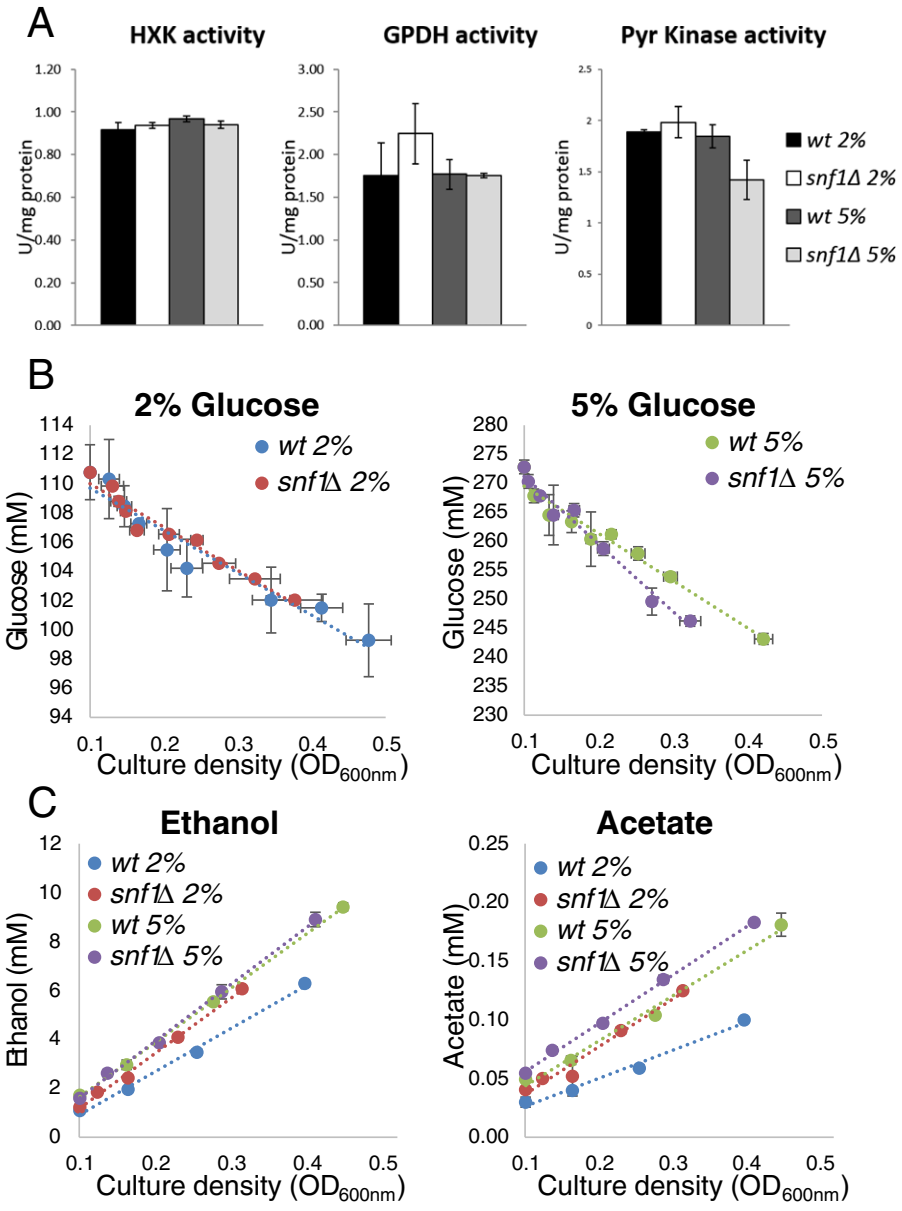

Fig. 2. Lack of Snf1 enhances secretion of glycolytic outputs. (A) Enzymatic activity of the indicated enzymes in total protein extracts. (B) Glucose consumption of *snf1Δ* and wt strains during exponential growth (culture density $OD_{600nm} = 0.1–0.5$) in 2% and 5% glucose, assayed by NMR analysis. (C) Ethanol and Acetate production of *snf1Δ* and wt cells in exponential phase of growth (culture density $OD_{600nm} = 0.1–0.5$) in 2% and 5% glucose, assayed by NMR analysis.

snf1Δ cells produced more glycolytic output products, *i.e.* ethanol and acetate, when growing in 2% glucose, but secreted the same amount of these metabolites as the wt when growing in 5% glucose (Fig. 2C).

These findings indicate that glycolysis is functionally enhanced in the absence of Snf1, in spite of unaltered glucose uptake, suggesting that the increased expression of glycolytic genes may be a transcriptional adaptation to the metabolic re-arrangement.

3.4. Growth in 5% glucose does not influence the snf1Δ fatty acid biosynthesis deregulation

One of the most extensively characterized phenotypes of *snf1Δ* cells is the accumulation of fatty acids, caused by the loss of Snf1-dependent phosphorylation of the acetyl-CoA carboxylase Acc1 [7,27]. This phenotype is of particular interest in the comparison between the metabolic roles of Snf1 and of its mammalian counterpart AMPK, which for other aspects diverged during evolution [28]. In yeast, loss of Snf1 and the consequent carbon overflow into the fatty acid biosynthetic pathway has been shown to cause inositol auxotrophy mediated by the impairment of *INO1* expression [27,29] and a depletion of the intracellular acetyl-CoA pool, causing a global reduction of histone acetylation [30]. However, no information about fatty acid biosynthesis in yeast at higher glucose concentration (>2%) is available.

We therefore quantitatively measured the fatty acid composition of wt and *snf1Δ* cells growing in 2% and 5% glucose by GC-MS analysis, to investigate whether the higher glucose supply (5% glucose) influences fatty acid accumulation in *snf1Δ*. As previously shown, lack of Snf1 caused accumulation of long chain fatty acids in 2% glucose and interestingly this happened also in cells growing in 5% glucose (Fig. 3).

It is well known that fatty acid elongation requires NADPH [31], so we speculated that in *snf1Δ* cells the reducing equivalents for fatty acid elongation could be obtained from the pentose-phosphate pathway. Nevertheless, when we measured the activity of glucose-6-phosphate dehydrogenase (coded by *ZWF1*), we failed to observe any

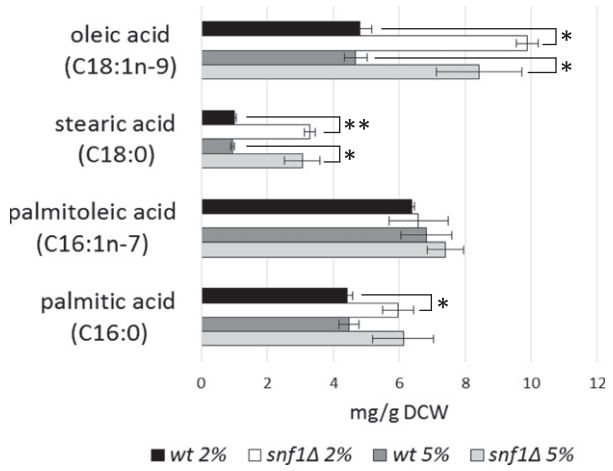

Fig. 3. Fatty acids are equally accumulated in 2% and 5% glucose *snf1Δ* log phase cells. The most abundant yeast long chain saturated (C16:0 and C:18:0) and un-saturated (C16:1n-7 and C18:1n-9) fatty acids were quantified from cells in exponential phase of growth (culture density $OD_{600nm} = 0.3$) by GC-MS analysis and normalized on cellular dry weight. *p-value < 0.05; **p-value < 0.005.

significant difference (Fig. S2A). However, our gene chip analysis evidenced that the genes coding for all the three NADH kinases (*POS5*, *UTR1*, *YEF1*) were up-regulated in *snf1Δ* cells growing in 2% glucose (Fig. S2B), thus suggesting a compensatory mechanism involving *de novo* NADPH biosynthesis.

3.5. Lack of Snf1 causes glutamate accumulation and fueling of carbon into the TCA cycle

Alteration of the Snf1 pathway in respiration-defective cells in stationary phase has been shown to cause a reshaping of the yeast metabolome, involving storage carbohydrates and amino acids [32]. To assess whether the observed alterations in both the glycolytic and the fatty acid biosynthetic pathways could be linked to broad alterations of the metabolism, we performed a metabolome profiling through ^{1}H-NMR spectroscopy, measuring a panel of intracellular metabolites. The most evident effect of the lack of Snf1 on metabolite levels in 2% glucose was the significant accumulation of glutamate, notably the most abundant metabolite (Fig. 4A). Interestingly, the accumulation of glutamate was reduced in cells growing in 5% glucose, correlating with the loss of the slow-growth phenotype of *snf1Δ* cells (Fig. 4A).

The profiling of intracellular amino acids also showed a slight but significant accumulation of intracellular methionine and a substantial reduction in the histidine content (Fig. 4A). The wt and *snf1Δ* strains did not show a differential histidine uptake from the media (data not shown) and the amino acid itself was supplemented in large excess, thus the observed reduction in histidine content is attributable only to the alteration of intracellular processes. The only specific utilization of histidine, except for protein synthesis, is its use as a precursor for thiamine biosynthesis. Thiamine, as thiamine diphosphate, is a cofactor in a number of biochemical reactions, but it is primarily required for the activity of pyruvate decarboxylase, pyruvate dehydrogenase and α-ketoglutarate dehydrogenase [33]. Hence, the enhanced glycolytic phenotype of *snf1Δ* cells may cause an enhanced thiamine utilization by pyruvate decarboxylase isoforms, thus accounting for the reduction in the intracellular histidine pool.

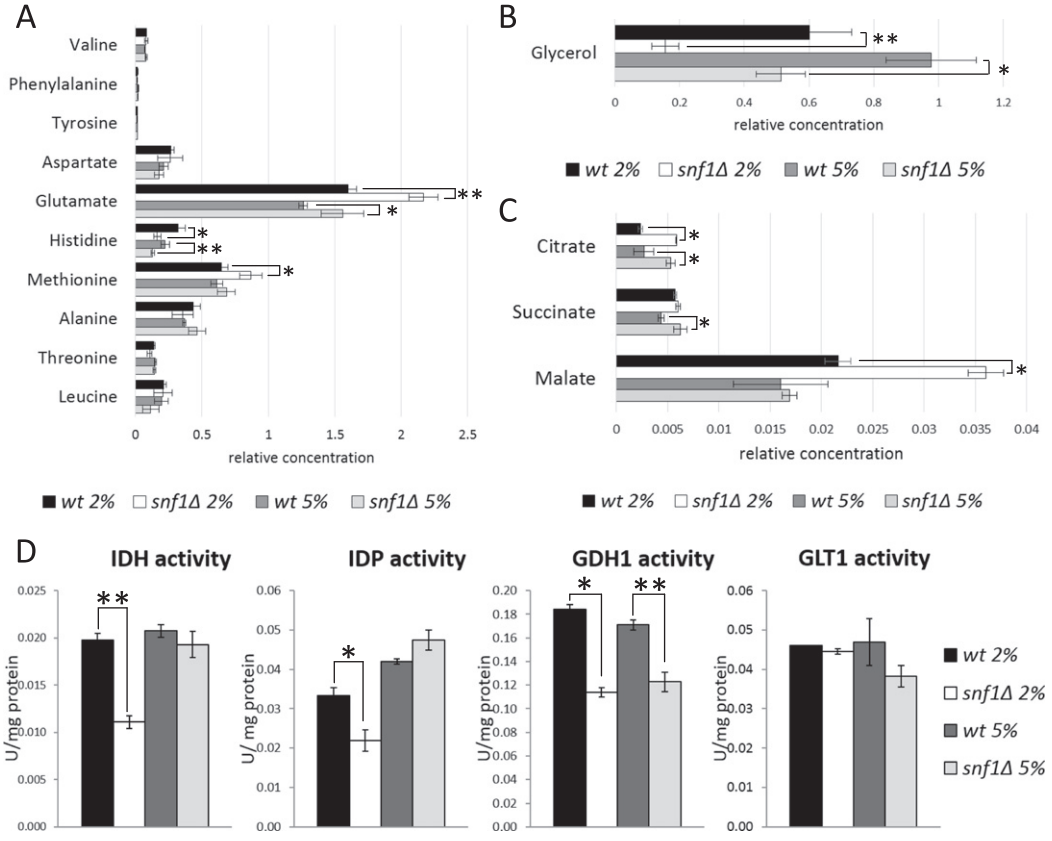

Fig. 4. Absence of Snf1 promotes carbon flow into the TCA cycle and glutamate accumulation. (A) Intracellular concentration of amino acids evaluated by NMR. *p-value < 0.05; **p-value < 0.005. (B) Intracellular concentration of glycerol evaluated by NMR. *p-value < 0.05; **p-value < 0.005. (C) Intracellular concentration of TCA cycle intermediates evaluated by GC-MS. *p-value < 0.05. (D) Enzymatic activity of the indicated enzymes in total protein extracts. *p-value < 0.05; **p-value < 0.005. All the experiments were performed with cells in exponential phase of growth (culture density $OD_{600nm} = 0.3$).

Another major alteration in *snf1Δ* cells was the 3-fold reduction in intracellular glycerol (Fig. 4B). This reduction was evident also for cells growing in 5% glucose, even if both wt and *snf1Δ* cells presented higher levels of glycerol in 5% glucose as compared to 2% glucose, consistent with the role of glycerol production as a redox valve to dispose excess cytosolic NADH during exponential growth [34]. Snf1 is known to phosphorylate and inactivate the major glycerol-3-phosphate dehydrogenase isoform Gpd2 in nutrient limited conditions [6], but here we show a reduction rather than an increase in glycerol content, indicating that this repressive role of the kinase is negligible in a non-limiting glucose concentration.

As mentioned above and shown in Fig. 4A, *snf1Δ* cells accumulate glutamate. In fermenting yeast cells the biosynthesis of glutamate occurs via the reaction of ammonia and α-ketoglutarate, thus it seems likely that cells accumulating this amino acid could increase the activity of the TCA cycle to supply biosynthetic building blocks. We therefore performed a targeted GC-MS analysis to measure intermediates of the TCA cycle and identified different levels of some of them in *snf1Δ* cells compared to the wt. In particular, *snf1Δ* cells accumulated more citrate both in 2% and 5% glucose, and even more clearly they accumulated malate when growing in 2% glucose (Fig. 4C), thus suggesting the hypothesis of an increased fueling of the TCA cycle in the absence of Snf1.

During growth on glucose, glutamate biosynthesis from α-ketoglutarate is performed mainly by the NADPH-dependent glutamate dehydrogenase Gdh1 [35]. We therefore measured the NADPH-dependent Gdh1 activity in total cell extracts, which interestingly was found lower in *snf1Δ* cells as compared to the wt (Fig. 4D). This finding was not surprising in light of the drain of NADPH caused by the enhanced fatty acid biosynthesis in a *snf1Δ* mutant (Fig. 4A), which adjusts the NADPH-consuming Gdh1 activity accordingly. Notably, this lower activity was consistent with the reduction of glycerol accumulation (Fig. 4B) and ethanol overproduction (Fig. 2C), matching the results previously obtained with *gdh1Δ* cells [36].

We also measured the activity of NAD- and NADP-dependent isocitrate dehydrogenases (IDH and IDP, respectively), which perform the synthesis of α-ketoglutarate from isocitrate and thus can be considered shared reactions between the TCA cycle and the glutamate biosynthetic pathway. Both enzymatic activities were lower in *snf1Δ* cells growing in 2% glucose, but the activities were not affected by deletion of Snf1 in 5% glucose (Fig. 4D). Besides, the activity of Glt1, the NADH-dependent glutamate synthase catalyzing the synthesis of two glutamate molecules from glutamine and α-ketoglutarate, was unaltered in *snf1Δ* cells (Fig. 4D). However this alternative glutamate biosynthetic pathway, which biochemically could account for glutamate accumulation, is evidently a hotspot, since all the genes coding for the enzymes of the pathway, in particular *GDH2*, were up-regulated in *snf1Δ* cells (Figs. S3A-B).

3.6. Increased uptake of amino acids in snf1Δ cells supports growth

The down-regulation of the main glutamate biosynthetic pathway through Gdh1 left unexplained the issue of the origin of the increased amount of glutamate in *snf1Δ* cells. We therefore tested the possibility of glutamate being a product of utilization of other amino acids assaying the consumption of leucine, methionine and histidine in the medium. While the consumption of histidine was negligible in every tested condition (data not shown), leucine and methionine uptake were significantly higher in *snf1Δ* cells growing in 2% glucose compared to the wt, consistently with the enhanced expression of genes encoding for amino acid transporters (Fig. S1B), while in 5% glucose the uptake of amino acids was comparable between the mutant strain and its control (Fig. 5A). Interestingly, leucine is known to be degraded through the Ehrlich pathway to glutamate and fusels alcohols [37] and *snf1Δ* cells transcriptionally up-regulate genes (*BAT2*, *THI3*, *ADH4*, *ADH5*) belonging to this pathway (Fig. S3C). Noteworthy, decreasing the concentration of leucine and methionine in the medium to 1/5th of the amount normally supplemented impaired the growth of *snf1Δ* cells only in 2% glucose, while having no effect on wt cells in this condition nor on wt and *snf1Δ* growing in 5% glucose (Fig. 5B). In keeping with this observation, the addition of leucine and methionine to a prototrophic *snf1Δ* strain increased its growth rate, while having no effect on the isogenic wt strain (Fig. S3D).

Strikingly, lowering the concentration of leucine and methionine in the medium abolished the accumulation of intracellular glutamate in *snf1Δ* cells growing in 2% glucose (Fig. 5C).

Altogether, these data support the hypothesis that *snf1Δ* cells in 2% glucose fuel carbon into the TCA cycle from amino acids supplemented in the medium.

3.7. Oxidative phosphorylation sustains growth and energy production in the absence of Snf1

The previous findings, that indicate an amino acid utilization through the TCA cycle in *snf1Δ* cells in 2% glucose, suggest a respiro-fermentative metabolism, thus requiring the re-oxidation of mitochondrial NADH, whose pool is well known to be separated from the cytoplasmic one [38]. To assess the role of mitochondrial activity, *snf1Δ* and wt cells in exponential phase of growth were treated with antimycin A, an inhibitor of the complex III of the electron transport chain. In 2% glucose the drug further impaired the slow growth phenotype of *snf1Δ* cells, without affecting wt cells (Fig. 6A). Remarkably, *snf1Δ* cells completely ceased to be affected by antimycin A when grown in 5% glucose (Fig. 6B). The same effect was observed in a *snf1Δ* strain with a different genetic background (Fig. S4A).

Electron flow through the respiratory chain ultimately leads to the synthesis of ATP, therefore we wondered whether the inhibition in a *snf1Δ* strain could influence energy supply. To assess this issue, we measured intracellular ATP content in wt and *snf1Δ* cells treated with antimycin A for 5 hours, as well as in mock controls. Although antimycin A treatment slightly reduced ATP content of wt cells, indicating a limited role of oxidative phosphorylation in wt fermenting cells, *snf1Δ* cells growing in 2% glucose synthesized a significantly larger fraction of their ATP through this mechanism (Fig. 6C). Consistently with the observed protective role of glucose on the growth of *snf1Δ* cells treated with antimycin A, ATP synthesis was not significantly affected in 5% glucose, as for the wt strain (Fig. 6C). In addition, *snf1Δ* cells contained lower basal ATP levels, indicating that unrequired energy consuming processes, possibly fatty acid biosynthesis, were draining energy.

Since a direct consequence of the inhibition of electron transport chain should be a reduction of the capability of mitochondrial NADH pool to be re-oxidized, we measured total NAD^+ and NADH intracellular content (mitochondrial and cytoplasmic) in the same conditions tested above for ATP content. *snf1Δ* cells contained significantly lower amounts of NAD when grown in 2% glucose, with a relative increase of the reduced form (Fig. 6D). After treatment with antimycin A, NADH in *snf1Δ* cells significantly increased, consistent with the predicted effect of electron transport chain inhibition (Fig. 6D). However, in the same condition NAD^+ content increased accordingly, indicating a compensatory mechanism probably involving the *de novo* NAD(H) biosynthesis. In agreement with the aforementioned results for growth and ATP, NAD^+/NADH levels of *snf1Δ* cells growing in 5% glucose were not influenced by antimycin A treatment (Fig. 6D). Remarkably, antimycin A treatment of *snf1Δ* cells grown with lower concentrations of leucine and methionine greatly impaired their growth, in respect to that of cells grown in standard medium (Fig. 6E). To further confirm the reliance of *snf1Δ* cells on respiration, we measured the oxygen consumption in our growth conditions. Strikingly, *snf1Δ* cells consumed a significantly increased amount of dissolved oxygen compared to the wt in 2% glucose (Fig. 6F). On the contrary, oxygen consumption of *snf1Δ* cells was not affected in 5% glucose (Fig. 6F).

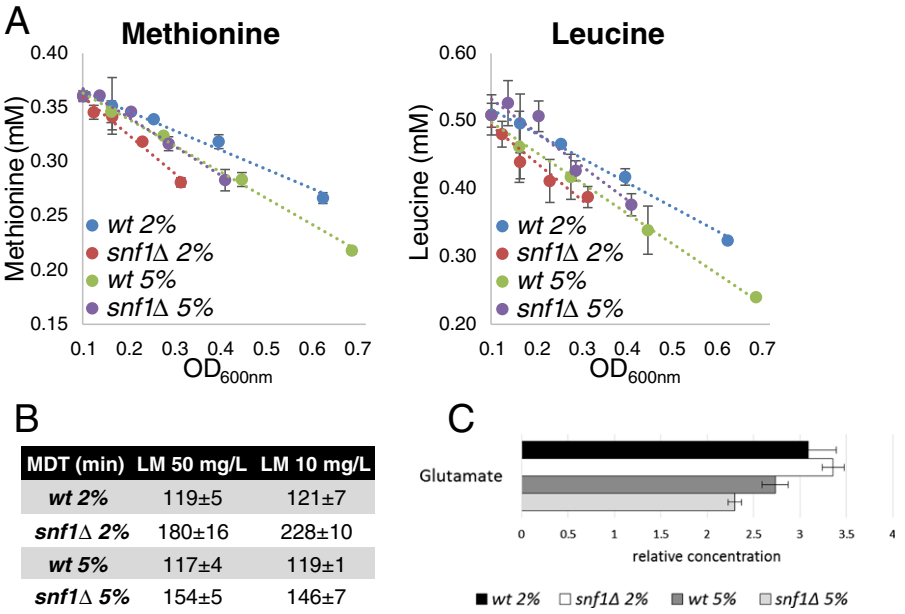

B

MDT (min)	LM 50 mg/L	LM 10 mg/L
wt 2%	119±5	121±7
snf1Δ 2%	180±16	228±10
wt 5%	117±4	119±1
snf1Δ 5%	154±5	146±7

Fig. 5. Enhanced amino acids uptake is necessary to sustain growth of *snf1Δ* cells. (A) Methionine and leucine consumption of *snf1Δ* and wt cells in exponential phase of growth (culture density $OD_{600nm} = 0.1–0.7$) in 2% and 5% glucose, assayed by NMR analysis. (B) Table showing the mean duplication time (MDT) of the indicated strains in standard medium (leucine and methionine 50 mg/L) or in amino acids limiting cultures (leucine and methionine 10 mg/L). (C) Glutamate intracellular content of the indicated strains in amino acids limiting cultures (leucine and methionine 10 mg/L) in exponential phase of growth (culture density $OD_{600nm} = 0.3$).

4. Discussion

Our work deepens the understanding of the involvement of signaling pathways in the regulation of metabolism of proliferating cells, by taking a snapshot of Snf1 deficient yeast cells without nutritional distress. Our analysis showed that even in condition of glucose availability, when Snf1 is only partially active (Fig. S4B), the lack of Snf1 causes rearrangements at multiple levels (summarized in Fig. 7), notably resembling the lack of proper AMPK activity in mammalian cells [39].

Recent studies provided evidence that the activation of AMPK is involved in growth control and tumorigenesis and that ablation of the catalytic subunit AMPKα1 promotes glucose uptake and aerobic glycolysis to support proliferation of cancer cells [28,40]. Recent phosphoproteomics data suggest that Snf1 might control glycolysis by phosphorylating phosphofructokinase and pyruvate dehydrogenase in glucose non-limiting conditions [41]. Here, we show that glycolysis of *snf1Δ* yeast cells is functionally enhanced (Fig. 2), with increased secretion into the medium of ethanol and acetate as compared to the wt, although no enhanced glucose consumption can be observed in 2% glucose. This enhanced glycolytic function is accompanied by transcriptional up-regulation of several genes of the pathway in *snf1Δ* cells growing in 2% glucose (Fig. 1), but we suggest that this could be an adaptation phenomenon induced by the metabolic changes, as observed also in mammalian cells [42]. Notably, it was recently observed that mutants of the Snf1 pathway present a thinner cell wall and a higher susceptibility to agents targeting this structure [43]. This effect is nicely reverted by deletion of *PFK1*, which restores the glucose-6-phosphate pool, which is reduced in *snf1Δ* cells. In light of our findings, we propose that the reduced accumulation of cell wall glucose derivatives could be due to the draining of glycolytic intermediates and their funneling to the ending products.

In proliferating cells, a conspicuous amount of carbon is diverted into lipids to support membrane biosynthesis and as biomass and energy reservoir [3]. Consistent with its role of keeper of cellular energy, AMPK has evolved as a negative regulator of fatty acids biosynthesis to avoid this energetically expensive process when nutrients are scarce [4] and this feature is conserved also in yeast cells [12,44]. In particular, both Snf1 and AMPK regulate the first step of fatty acid biosynthesis in a conserved way by direct phosphorylation of acetyl-CoA carboxylase (Acc1 and ACC1, respectively) [7,29,45]. Noteworthy, yeast exclusively use acetate activated in the cytoplasm to provide acetyl-CoA for fatty acids synthesis, since unlike plants and animals it lacks the citrate lyase activity to fuel this process through the TCA cycle [46]. Therefore, given that yeast fully relies on glycolysis for this process, we propose that *snf1Δ* cells need to increase the glycolysis (Fig. 2) to sustain the hyper-accumulation of fatty acids (Fig. 3).

The synthesis of fatty acids is not only expensive in terms of carbon and energy, but it also exploits the reducing equivalent (NADPH) pool of the cell [31], therefore it is likely that *snf1Δ* cells face a problem in balancing its NADPH/$NADP^+$ ratio. Even if the pentose-phosphate shunt is the main pathway for $NADP^+$ reduction, it is disadvantageous for energy generation and we lack direct evidence of its enhancement in *snf1Δ* cells. Instead, the limited NADPH pool probably drives *snf1Δ* cells to down-regulate the processes which utilize the cofactor, as we show for glutamate biosynthesis via Gdh1 (Fig. 4D). Interestingly, excessive glutamate is known to activate its degradation to succinate via γ-aminobutyric acid (GABA), involving the reduction of $NADP^+$ to NADPH [47]. Therefore, it is possible that this phenomenon is occurring in *snf1Δ* cells, concomitantly obtaining NADPH and fueling the TCA cycle.

In the absence of glucose, Snf1 negatively regulates the translation of the transcription factor Gcn4, thus inhibiting the expression of a regulon of genes involved in amino acids biosynthesis, as firstly reported by Shirra and coauthors [10]. In our gene chip analysis, that regulon is de-repressed even in *snf1Δ* cells growing in 2% glucose, suggesting that Snf1 effect on Gcn4 can be extended also to non-limiting nutrient conditions (Fig. S1B). Furthermore, we show that alterations of amino acids metabolism are actually relevant for *snf1Δ* cells, the most evident being a significant intracellular accumulation of glutamate (Fig. 4A). Glutamate is pivotal in the biosynthesis of many other amino acids, and conversely it is one of the products of their degradation. Amino acids supplemented in the medium can be used by the cells not only as nitrogen source, but also as carbon source, via degradation to glutamate, and this has been described especially for leucine and methionine [48,49]. In this framework, the reliance of *snf1Δ* cells on leucine and methionine uptake (Fig. 5A) demonstrated by the impairment of

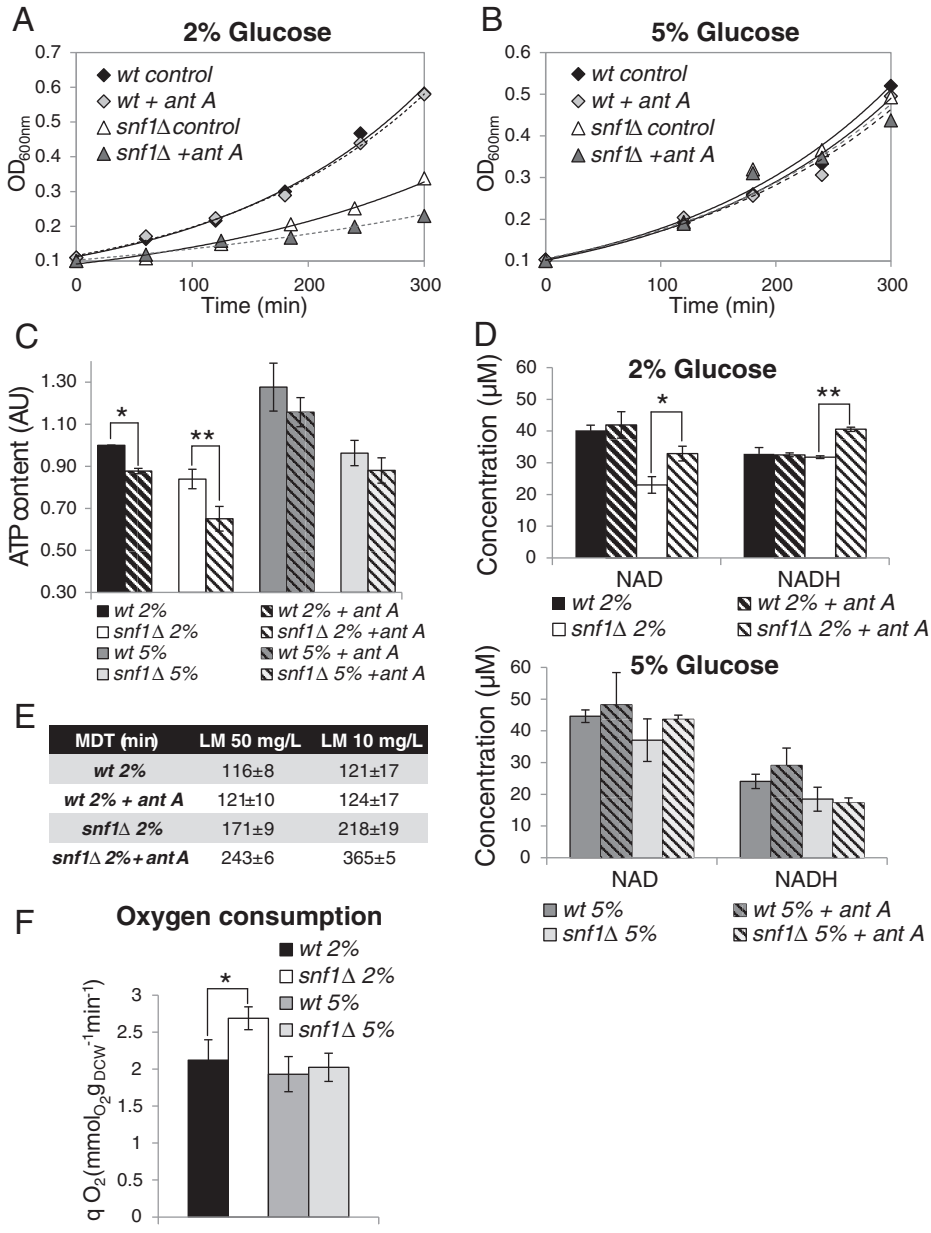

MDT (min)	LM 50 mg/L	LM 10 mg/L
wt 2%	116±8	121±17
wt 2% + ant A	121±10	124±17
snf1Δ 2%	171±9	218±19
snf1Δ 2%+antA	243±6	365±5

Fig. 6. *snf1Δ* cells require oxidative phosphorylation to sustain growth and generate ATP. (A) Growth curve of wt and *snf1Δ* cells in exponential phase (culture density OD_{600nm} = 0.1-0.6) in 2% glucose treated and un-treated with antimycin A. (B) Growth curve of wt and *snf1Δ* cells in exponential phase (culture density OD_{600nm} = 0.1–0.6) in 5% glucose treated and un-treated with antimycin A. (C) Intracellular ATP concentration of the indicated strains after 5 hours treatment with antimycin A, un-treated sample shown as mock control. *p-value < 0.05; **p-value < 0.005. (D) Intracellular content of NAD and NADH of the indicated strains after 5 hours treatment with antimycin A, un-treated sample shown as mock control. *p-value < 0.05; **p-value < 0.005. (E) Table showing the mean duplication time (MDT) of wt and *snf1Δ* cells either treated or not with antimycin A and growing in standard medium (leucine and methionine 50 mg/L) or in amino acids limiting conditions (leucine and methionine 10 mg/L). (F) Oxygen consumption of the indicated strains in exponential phase of growth (culture density OD_{600nm} = 0.5) expressed as qO_2 ($mmol_{oxygen}\ g^{-1}_{dry\ weight}\ min^{-1}$). *p-value < 0.05.

growth when these amino acids are reduced in the medium containing 2% glucose (Fig. 5B), links leucine and methionine assimilation to compensation of carbon and energy waste (Fig. 7). Remarkably, methionine-dependence occurs in many human tumors and methionine-free diet greatly reduces tumor growth in preclinical models [50].

Utilization of glutamate as carbon source requires its conversion to α-ketoglutarate and this process seems to be favored in *snf1Δ* cells at least at the transcriptional level (Fig. S3A-B). Continuation of this process essentially requires the execution of a part of the TCA cycle, in keeping with the accumulation of malate in *snf1Δ* cells (Fig. 4C). Moreover, inhibition of re-oxidation of mitochondrial NADH (treating with antimycin A) is detrimental for *snf1Δ* cells in 2% glucose, since it coordinately affects growth, ATP and NAD^+/NADH contents (Fig. 6). Re-oxidation of mitochondrial NADH requires the activity of the respiratory chain and the final reduction of O_2. Indeed, *snf1Δ* cells growing in 2% glucose showed an increased oxygen consumption (Fig. 6F). It was recently reported that Snf1 is required to overcome the impaired respiratory function caused by loss of mitochondrial DNA in stationary phase [32]. Our findings complement this notion, indicating that lack of Snf1 causes an increase of cellular dependence of mitochondrial function.

The common feature of the phenotypes described for *snf1Δ* cells in this paper is that they are almost undetectable when cells grow in the presence of 5% glucose. Even if 2% glucose is non-limiting for fermentative growth, increase of glucose concentration to 5% results in enhanced secretion of fermentation metabolites in wt cells (Fig. 2C). In addition, glucose uptake is higher in *snf1Δ* cells grown in 5% glucose (Fig. 2B).

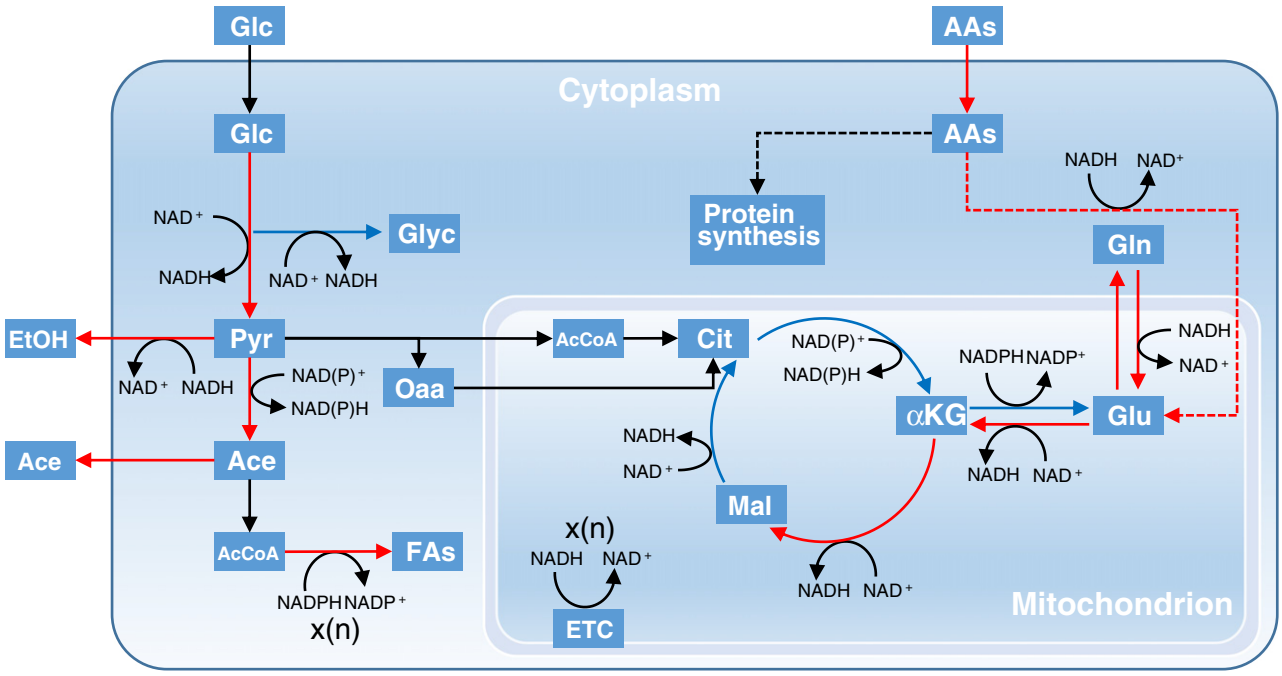

Fig. 7. Map of the metabolic rewiring occurring upon Snf1 loss. Schematization of the metabolic rewiring occurring upon Snf1 loss. Red and blue arrows indicate processes for which there is evidence at different levels (transcriptional, enzymatic, product concentration) of enhancement or reduction, respectively.

This finding strongly suggests that enhanced glucose metabolism satisfies the requirements of *snf1Δ* cells and abolishes their reliance on amino acids utilization. Noteworthy, *snf1Δ* cells have been shown to have impaired intracellular acetyl-CoA levels and subsequently reduced histone acetylation, a phenotype that could be at least partially reverted by the replenishment of acetyl-CoA pool [30]. Increased carbon flux provided in 5% glucose could therefore account for increased supply of acetyl-CoA, which, as described above, is directly subtracted for fatty acids biosynthesis [46]. This could relieve *snf1Δ* cells from effects of reduced histone acetylation on gene expression, which has been pointed out as particularly important at growth genes such as Cln3 [51]. This hypothesis well fits our previous findings of *snf1Δ* cells having a cell cycle defect in the G_1 to S transition, accompanied by the impairment of the transcription of G_1-specific genes [13,14].

In conclusion, here we describe the rewiring occurring in the metabolic network of cells lacking Snf1, showing remarkable resemblances with mammalian cells deprived of AMPK and identifying a strategy adopted by these cells to guarantee growth. It has been pointed out that although AMPK loss of function alone is not sufficient to cause transformation, mutations of the kinase are not infrequent in cancers [39]. However, lack of functional AMPK causes ambivalent effects, because despite the loss of its catalytic activity enhances tumorigenesis, it also deprives the cells of a critical pathway for the response to environmental stresses. It is not surprising, therefore, that AMPK has been indicated as a target for cancer therapy [52]. In this work we establish the usefulness of yeast in the study of a signaling pathway which until now showed marginal similarities with its relative in higher eukaryotes. Remarkably, the metabolic strategies adopted by Snf1/AMPK deficient cells to support proliferation, as the increase of the utilization of amino acids as carbon source reported here, are reminiscent of the increased glutamine utilization that is the hallmark of several cancer cells [53].

Conflict of interest

The authors declare that they have no conflict of interest.

Transparency document

The Transparency document associated with this article can be found, in the online version.

Acknowledgments

The authors would like to thank S. Busti for fruitful discussion and A. Castoldi for performing preliminary experiments. This work has been supported by grants to P. Coccetti from the Italian Government (FAR) and to P. Coccetti and L. Alberghina from the SysBioNet project, a MIUR initiative from the Italian Roadmap of European Strategy Forum on Research Infrastructures (ESFRI). R.N. and F.T. have been supported by fellowships from MIUR, V.R. and C.G. from SysBioNet. Funding from the Knut and Alice Wallenberg Foundation and the Novo Nordisk Foundation is acknowledged.

Appendix A. Supplementary data

Supplementary data to this article can be found online at http://dx.doi.org/10.1016/j.bbamcr.2015.03.014.

References

[1] P. Jorgensen, M. Tyers, How cells coordinate growth and division, Curr. Biol. 14 (2004) R1014–R1027, http://dx.doi.org/10.1016/j.cub.2004.11.027.
[2] J.J. Turner, J.C. Ewald, J.M. Skotheim, Cell size control in yeast, Curr. Biol. 22 (2012) R350–R359, http://dx.doi.org/10.1016/j.cub.2012.02.041.
[3] M.G. Vander Heiden, L.C. Cantley, C.B. Thompson, Understanding the Warburg effect: the metabolic requirements of cell proliferation, Science 324 (2009) 1029–1033, http://dx.doi.org/10.1126/science.1160809.
[4] D.G. Hardie, AMP-activated/SNF1 protein kinases: conserved guardians of cellular energy, Nat. Rev. Mol. Cell Biol. 8 (2007) 774–785, http://dx.doi.org/10.1038/nrm2249.
[5] K. Hedbacker, M. Carlson, SNF1/AMPK pathways in yeast, Front. Biosci. 13 (2008) 2408–2420.
[6] Y.J. Lee, G.R. Jeschke, F.M. Roelants, J. Thorner, B.E. Turk, Reciprocal phosphorylation of yeast glycerol-3-phosphate dehydrogenases in adaptation to distinct types of stress, Mol. Cell. Biol. 32 (2012) 4705–4717, http://dx.doi.org/10.1128/MCB.00897-12.

[7] S. Shi, Y. Chen, V. Siewers, J. Nielsen, Improving production of malonyl coenzyme A-derived metabolites by abolishing Snf1-dependent regulation of Acc1, MBio. 5 (2014) e01130–14, http://dx.doi.org/10.1128/mBio.01130-14.

[8] M.A. Treitel, S. Kuchin, M. Carlson, Snf1 protein kinase regulates phosphorylation of the Mig1 repressor in Saccharomyces cerevisiae, Mol. Cell. Biol. 18 (1998) 6273–6280.

[9] J. Zhang, S. Vaga, P. Chumnanpuen, R. Kumar, G.N. Vemuri, R. Aebersold, et al., Mapping the interaction of Snf1 with TORC1 in Saccharomyces cerevisiae, Mol. Syst. Biol. 7 (2011) 545, http://dx.doi.org/10.1038/msb.2011.80.

[10] M.K. Shirra, R.R. McCartney, C. Zhang, K.M. Shokat, M.C. Schmidt, K.M. Arndt, A chemical genomics study identifies Snf1 as a repressor of GCN4 translation, J. Biol. Chem. 283 (2008) 35889–35898, http://dx.doi.org/10.1074/jbc.M805325200.

[11] E.M. Humston, K.M. Dombek, J.C. Hoggard, E.T. Young, R.E. Synovec, Time-dependent profiling of metabolites from Snf1 mutant and wild type yeast cells, Anal. Chem. 80 (2008) 8002–8011, http://dx.doi.org/10.1021/ac800998j.

[12] R. Usaite, M.C. Jewett, A.P. Oliveira, J.R. Yates, L. Olsson, J. Nielsen, Reconstruction of the yeast Snf1 kinase regulatory network reveals its role as a global energy regulator, Mol. Syst. Biol. 5 (2009) 319, http://dx.doi.org/10.1038/msb.2009.67.

[13] S. Pessina, V. Tsiarentsyeva, S. Busnelli, M. Vanoni, L. Alberghina, P. Coccetti, Snf1/AMPK promotes S-phase entrance by controlling CLB5 transcription in budding yeast, Cell Cycle 9 (2010) 2189–2200.

[14] S. Busnelli, F. Tripodi, R. Nicastro, C. Cirulli, G. Tedeschi, R. Pagliarin, et al., Snf1/AMPK promotes SBF and MBF-dependent transcription in budding yeast, Biochim. Biophys. Acta 1833 (2013) 3254–3264, http://dx.doi.org/10.1016/j.bbamcr.2013.09.014.

[15] R.A. Irizarry, B. Hobbs, F. Collin, Y.D. Beazer-Barclay, K.J. Antonellis, U. Scherf, et al., Exploration, normalization, and summaries of high density oligonucleotide array probe level data, Biostatistics 4 (2003) 249–264, http://dx.doi.org/10.1093/biostatistics/4.2.249.

[16] C. Airoldi, F. Tripodi, C. Guzzi, R. Nicastro, P. Coccetti, NMR analysis of budding yeast metabolomics: a rapid method for sample preparation, Mol. Biosyst. 11 (2015) 379–383, http://dx.doi.org/10.1039/c4mb00452c.

[17] S. Khoomrung, P. Chumnanpuen, S. Jansa-ard, I. Nookaew, J. Nielsen, Fast and accurate preparation fatty acid methyl esters by microwave-assisted derivatization in the yeast Saccharomyces cerevisiae, Appl. Microbiol. Biotechnol. 94 (2012) 1637–1646, http://dx.doi.org/10.1007/s00253-012-4125-x.

[18] H. Bergmeyer, M. Grassl, H. Walter, Methods of enzymatic analysis, 3rd ed. Verlag Chemie, 1983.

[19] M.L. Delgado, J.E. O'Connor, I. Azorín, J. Renau-Piqueras, M.L. Gil, D. Gozalbo, The glyceraldehyde-3-phosphate dehydrogenase polypeptides encoded by the Saccharomyces cerevisiae TDH1, TDH2 and TDH3 genes are also cell wall proteins, Microbiology 147 (2001) 411–417.

[20] E.A. Noltmann, C.J. Gubler, S.A. Kuby, Glucose 6-phosphate dehydrogenase (Zwischenferment). I. Isolation of the crystalline enzyme from yeast. J. Biol. Chem. 236 (1961) 1225–1230.

[21] R.M. Chell, T.K. Sundaram, A.E. Wilkinson, Isolation and characterization of isocitrate lyase from a thermophilic Bacillus sp, Biochem. J. 173 (1978) 165–177.

[22] C. Cogoni, L. Valenzuela, D. González-Halphen, H. Olivera, G. Macino, P. Ballario, et al., Saccharomyces cerevisiae has a single glutamate synthase gene coding for a plant-like high-molecular-weight polypeptide, J. Bacteriol. 177 (1995) 792–798.

[23] H. Shimizu, T. Kuratsu, F. Hirata, Purification and some properties of glutamate dehydrogenase from *Proteus inconstans*, J. Ferment. Technol. 57 (1979) 428–433.

[24] I. Ferrero, A.M. Viola, A. Goffeau, Induction by glucose of an antimycin-insensitive, azide-sensitive respiration in the yeast Kluyveromyces lactis, Antonie Van Leeuwenhoek 47 (1981) 11–24.

[25] H. Sasaki, T. Kishimoto, T. Mizuno, T. Shinzato, H. Uemura, Expression of GCR1, the transcriptional activator of glycolytic enzyme genes in the yeast Saccharomyces cerevisiae, is positively autoregulated by Gcr1p, Yeast 22 (2005) 305–319, http://dx.doi.org/10.1002/yea.1212.

[26] L. Tomás-Cobos, P. Sanz, Active Snf1 protein kinase inhibits expression of the *Saccharomyces cerevisiae* HXT1 glucose transporter gene, Biochem. J. 368 (2002) 657–663, http://dx.doi.org/10.1042/BJ20020984.

[27] H.F. Hofbauer, F.H. Schopf, H. Schleifer, O.L. Knittelfelder, B. Pieber, G.N. Rechberger, et al., Regulation of gene expression through a transcriptional repressor that senses acyl-chain length in membrane phospholipids, Dev. Cell 29 (2014) 729–739, http://dx.doi.org/10.1016/j.devcel.2014.04.025.

[28] B. Faubert, G. Boily, S. Izreig, T. Griss, B. Samborska, Z. Dong, et al., AMPK is a negative regulator of the Warburg effect and suppresses tumor growth in vivo, Cell Metab. 17 (2013) 113–124, http://dx.doi.org/10.1016/j.cmet.2012.12.001.

[29] M.K. Shirra, J. Patton-Vogt, A. Ulrich, O. Liuta-Tehlivets, S.D. Kohlwein, S.A. Henry, et al., Inhibition of acetyl coenzyme A carboxylase activity restores expression of the INO1 gene in a snf1 mutant strain of *Saccharomyces cerevisiae*, Mol. Cell. Biol. 21 (2001) 5710–5722.

[30] M. Zhang, L. Galdieri, A. Vancura, The yeast AMPK homolog SNF1 regulates acetyl coenzyme A homeostasis and histone acetylation, Mol. Cell. Biol. 33 (2013) 4701–4717, http://dx.doi.org/10.1128/MCB. 00198-13.

[31] O. Tehlivets, K. Scheuringer, S.D. Kohlwein, Fatty acid synthesis and elongation in yeast, Biochim. Biophys. Acta 1771 (2007) 255–270, http://dx.doi.org/10.1016/j.bbalip.2006.07.004.

[32] R.M.N. Friis, J.P. Glaves, T. Huan, L. Li, B.D. Sykes, M.C. Schultz, Rewiring AMPK and mitochondrial retrograde signaling for metabolic control of aging and histone acetylation in respiratory-defective cells, Cell Rep. 7 (2014) 565–574, http://dx.doi.org/10.1016/j.celrep.2014.03.029.

[33] E. Kowalska, A. Kozik, The genes and enzymes involved in the biosynthesis of thiamin and thiamin diphosphate in yeasts, Cell. Mol. Biol. Lett. 13 (2008) 271–282, http://dx.doi.org/10.2478/s11658-007-0055-5.

[34] R. Ansell, K. Granath, S. Hohmann, J.M. Thevelein, L. Adler, The two isoenzymes for yeast NAD + -dependent glycerol 3-phosphate dehydrogenase encoded by GPD1 and GPD2 have distinct roles in osmoadaptation and redox regulation, EMBO J. 16 (1997) 2179–2187, http://dx.doi.org/10.1093/emboj/16.9.2179.

[35] A. DeLuna, A. Avendano, L. Riego, A. Gonzalez, NADP-glutamate dehydrogenase isoenzymes of *Saccharomyces cerevisiae*. Purification, kinetic properties, and physiological roles. J. Biol. Chem. 276 (2001) 43775–43783, http://dx.doi.org/10.1074/jbc.M107986200.

[36] C. Bro, B. Regenberg, J. Nielsen, Genome-wide transcriptional response of a *Saccharomyces cerevisiae* strain with an altered redox metabolism, Biotechnol. Bioeng. 85 (2004) 269–276, http://dx.doi.org/10.1002/bit.10899.

[37] J.R. Dickinson, Pathways of leucine and valine catabolism in yeast, Methods Enzymol. 324 (2000) 80–92.

[38] M. Kato, S.-J. Lin, Regulation of NAD+ metabolism, signaling and compartmentalization in the yeast Saccharomyces cerevisiae, DNA Repair (Amst) (2014)http://dx.doi.org/10.1016/j.dnarep.2014.07.009.

[39] B. Faubert, E.E. Vincent, M.C. Poffenberger, R.G. Jones, The AMP-activated protein kinase (AMPK) and cancer: Many faces of a metabolic regulator, Cancer Lett. (2014)http://dx.doi.org/10.1016/j.canlet.2014.01.018.

[40] B. Faubert, E.E. Vincent, T. Griss, B. Samborska, S. Izreig, R.U. Svensson, et al., Loss of the tumor suppressor LKB1 promotes metabolic reprogramming of cancer cells via HIF-1α, Proc. Natl. Acad. Sci. U. S. A. 111 (2014) 2554–2559, http://dx.doi.org/10.1073/pnas.1312570111.

[41] K.A. Braun, S. Vaga, K.M. Dombek, F. Fang, S. Palmisano, R. Aebersold, et al., Phosphoproteomic analysis identifies proteins involved in transcription-coupled mRNA decay as targets of Snf1 signaling, Sci. Signal. 7 (2014) ra64, http://dx.doi.org/10.1126/scisignal.2005000.

[42] E. Roche, F. Assimacopoulos-Jeannet, L.A. Witters, B. Perruchoud, G. Yaney, B. Corkey, et al., Induction by glucose of genes coding for glycolytic enzymes in a pancreatic beta-cell line (INS-1), J. Biol. Chem. 272 (1997) 3091–3098.

[43] K. Backhaus, D. Rippert, C.J. Heilmann, A.G. Sorgo, C.G. de Koster, F.M. Klis, et al., Mutations in SNF1 complex genes affect yeast cell wall strength, Eur. J. Cell Biol. 92 (2013) 383–395, http://dx.doi.org/10.1016/j.ejcb.2014.01.001.

[44] E. Borklu Yucel, K.O. Ulgen, Assessment of crosstalks between the Snf1 kinase complex and sphingolipid metabolism in S. cerevisiae via systems biology approaches, Mol. Biosyst. 9 (2013) 2914–2931, http://dx.doi.org/10.1039/c3mb70248k.

[45] S.P. Davies, A.T. Sim, D.G. Hardie, Location and function of three sites phosphorylated on rat acetyl-CoA carboxylase by the AMP-activated protein kinase, Eur. J. Biochem. 187 (1990) 183–190.

[46] M.J. Hynes, S.L. Murray, ATP-citrate lyase is required for production of cytosolic acetyl coenzyme A and development in Aspergillus nidulans, Eukaryot. Cell 9 (2010) 1039–1048, http://dx.doi.org/10.1128/EC.00080-10.

[47] F. Ramos, M. el Guezzar, M. Grenson, J.M. Wiame, Mutations affecting the enzymes involved in the utilization of 4-aminobutyric acid as nitrogen source by the yeast Saccharomyces cerevisiae, Eur. J. Biochem. 149 (1985) 401–404.

[48] P. Perpète, O. Duthoit, S. De Maeyer, L. Imray, A.I. Lawton, K.E. Stavropoulos, et al., Methionine catabolism in *Saccharomyces cerevisiae*, FEMS Yeast Res. 6 (2006) 48–56, http://dx.doi.org/10.1111/j.1567-1356.2005.00005.x.

[49] J.S. Hothersall, A. Ahmed, Metabolic fate of the increased yeast amino Acid uptake subsequent to catabolite derepression, J. Amino Acids 2013 (2013) 461901, http://dx.doi.org/10.1155/2013/461901.

[50] Y. Hoshiya, H. Guo, T. Kubota, T. Inada, F. Asanuma, Y. Yamada, et al., Human tumors are methionine dependent in vivo, Anticancer Res. 15 (1995) 717–718.

[51] L. Shi, B.P. Tu, Acetyl-CoA induces transcription of the key G1 cyclin CLN3 to promote entry into the cell division cycle in *Saccharomyces cerevisiae*, Proc. Natl. Acad. Sci. U. S. A. 110 (2013) 7318–7323, http://dx.doi.org/10.1073/pnas.1302490110.

[52] D.G. Hardie, AMPK: a target for drugs and natural products with effects on both diabetes and cancer, Diabetes 62 (2013) 2164–2172, http://dx.doi.org/10.2337/db13-0368.

[53] L. Alberghina, D. Gaglio, Redox control of glutamine utilization in cancer, Cell Death Dis. 5 (2014) e1561, http://dx.doi.org/10.1038/cddis.2014.513.